Zonal jets in equilibrating baroclinic instability on the polar beta-plane: experiments with altimetry

Y. D. Afanasyev

Memorial University of Newfoundland, St. John's, Canada

1. Introduction

Results from the laboratory experiments on the evolution of baroclinically unstable flows generated in a rotating tank with topographic β-effect are presented. We study zonal jets of alternating direction which occur in these flows. The primary system we model includes lighter fluid in the South and heavier fluid in the North with resulting slow meridional circulation and fast mean zonal motion. We model two-layer system for simplicity. Velocity shear between the layers results in baroclinic instability which equilibrates and, due to interaction with β-effect generates zonal jets. This system is archetypal for various geophysical systems including the general circulation and jet streams in the Earth's atmosphere, the Antarctic Circumpolar Current (Thompson 2008) or the areas in the vicinity of western boundary currents where baroclinic instability and multiple zonal jets are observed (Maximenko et al. 2005).

2. Laboratory technique

In our experiments, we measure the surface elevation, η, and the thickness of the upper layer, h_1, using the Altimetric Imaging Velocimetry (AIV) and the Optical Thickness Velocimetry (OTV) techniques respectively (for more details see Afanasyev et al. 2009). The velocity of the flow can then be either obtained in a geostrophic approximation

$$\mathbf{V}_g = \frac{g}{f_0}\left(\mathbf{n}\times\nabla\eta\right), \tag{1}$$

or in a quasi-geostrophic (QG) approximation

$$\mathbf{V} = \mathbf{V}_g - \frac{g}{f_o^2}\frac{\partial}{\partial t}\nabla\eta - \frac{g^2}{f_o^3}J\left(\eta,\nabla\eta\right), \tag{2}$$

where **n** is the vertical unit vector, **V** is the horizontal velocity vector and f_0 is the Coriolis parameter. While the measured surface slope is precise (within the experimental error, of course), the "textbook" criteria of validity of the geostrophic or QG approximations applies for velocity. The velocity, given by Eqs. (1) or (2) is, in fact, a barotropic velocity of the flow.

Baroclinic geostrophic velocity due to the variation of the thickness of the layer can be obtained as

$$\mathbf{V}_{gbc} = -\frac{g'}{f_o}\left(\boldsymbol{n}\times\nabla h_1\right), \tag{3}$$

where $g' = g\left(\rho_2 - \rho_1\right)/\rho_1$ is the reduced gravity, ρ_1 and ρ_2 are the densities of the upper and lower layer respectively. QG baroclinic velocity, $\mathbf{V}_{bc}$, can be obtained similar from Eq. (2) by substituting η by $-h_1$.

Thus, the velocity in the upper layer is equal to the barotropic velocity, $\mathbf{v}_1 = \mathbf{V}$, while the velocity in the lower layer is given by the sum of the barotropic and baroclinic velocities, $\mathbf{v}_2 = \mathbf{V} + \mathbf{V}_{bc}$.

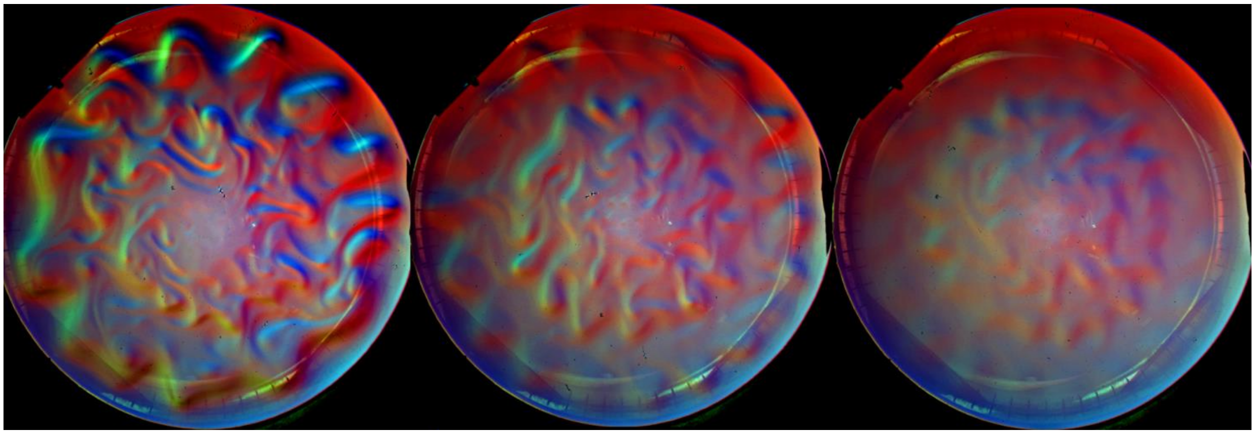

Figure 1. Evolution of a baroclinically unstable flow on the polar β-plane. The flow is visualized by AIV.

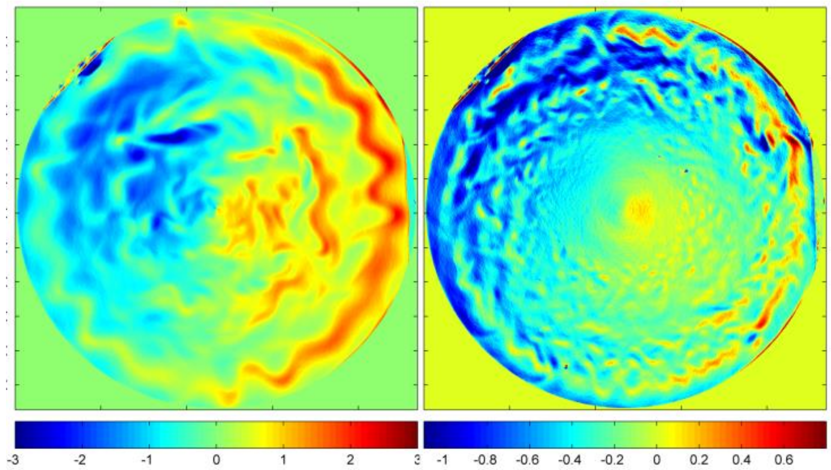

Figure 2. Azimuthal velocity in the experiments with salinity S = 30 ppt and S = 10 ppt.

3. Results

The flows were generated by a source of fresh water located along the wall of the tank at the surface of saline water layer. The source of fresh water creates a strong coastal current which flows counterclockwise such that the wall is on its right (Figure 1). The current is unstable with respect to a baroclinic/frontal instability and forms meanders. The current encircles the tank; the fresh water supplied by the source, gradually fills the interior of the tank. As a result, a fresh water layer forms at the surface, on top of the saline layer. By the time when the forcing is stopped, the fresh water covers the entire area of the tank. After that, the flow continues to evolve, albeit more slowly. Mean circulation in both the top and bottom layers is easy to understand. The surface is slightly elevated near the wall. As a result, the coastal current in the upper layer flows in the cyclonic direction such that a simple balance between the Coriolis force directed towards the wall and the pressure gradient acting in the opposite direction, is maintained. The upper layer is thicker at the wall of the tank than in its center (it adjusts towards a layer of uniform thickness on a very long time scale). The pressure in the lower layer is relatively low near the wall because of the relatively thick layer of (lighter) fresh water on top and relatively high in the center of the tank. Simple geostrophy then suggests that an anticyclonic gyre must be created in the lower layer. Thus, the top and bottom layers rotate in the opposite directions. The velocity shear is created and maintained by the baroclinic structure of the two-layer system. Theory predicts that a velocity shear in combination with the density difference between the layers should result in a baroclinic instability. Indeed, the instability was observed in all of our experiments; it persisted for a long time after the forcing stopped.

Baroclinic instability continuously creates meanders and filaments which protrude in the meridional (radial) direction (or rather at some angle to a meridian). Figure 1 shows that long narrow filaments are a dominant feature of the flow. The meridional motion of the filaments is affected by the β-effect. As a result, zonal jets are formed. Zonal jets were observed to be a robust feature in our experiments (Figure 2). Herein, we analyze the forcing of the jets by meanders, filaments and eddies created in the baroclinically unstable flow. This forcing is usually called "eddy forcing"; it is described statistically by presenting the flow in terms of its mean characteristics and perturbations without regard to a particular character of the perturbations. In a two-layer system, the mean zonal momentum balance in the statistically steady state is given by

$$\frac{\partial \overline{u}_n}{\partial t} \approx \begin{cases} -\dfrac{D_{1.5}}{\overline{h}_1} - \dfrac{\partial R_1}{\partial y}, & n=1 \\ \dfrac{D_{1.5}}{\overline{h}_2} - \dfrac{\partial R_2}{\partial y} - f_{bot}, & n=2 \end{cases} , \tag{4}$$

where overbar denotes time mean values, $\overline{h}_1$ and $\overline{h}_2$ are the thicknesses of the upper and lower layer respectively and eddy fluxes are defined as

$$D_{1.5} = -f_0 \overline{v'_{1.5}\eta'_{1.5}} , \tag{5}$$

$$R_n = \overline{u'_n v'_n} . \tag{6}$$

Index 1.5 refers to the quantities at the interface between the layers; $v_{1.5} = (v_1 + v_2)/2$ and $\eta'_{1.5} = \overline{h}_1 - h_1$ is the elevation of the interface. $D_{1.5}$ is the form drag which occurs because of the undulated interface. The form drag describes the exchange of momentum between the layers; when one layer is accelerated by this term, another layer is decelerated. R_n is the Reynolds stress and the forcing is given by its horizontal divergence. The term f_{bot} in Eq. (4) represents the bottom Ekman friction. Friction due to regular viscosity is not included in Eq. (4) but is certainly a factor in both layers. In a steady state there is no acceleration, $\partial \overline{u}_n / \partial t = 0$, and the right-hand side of Eq. (4) must be balanced in both layers.

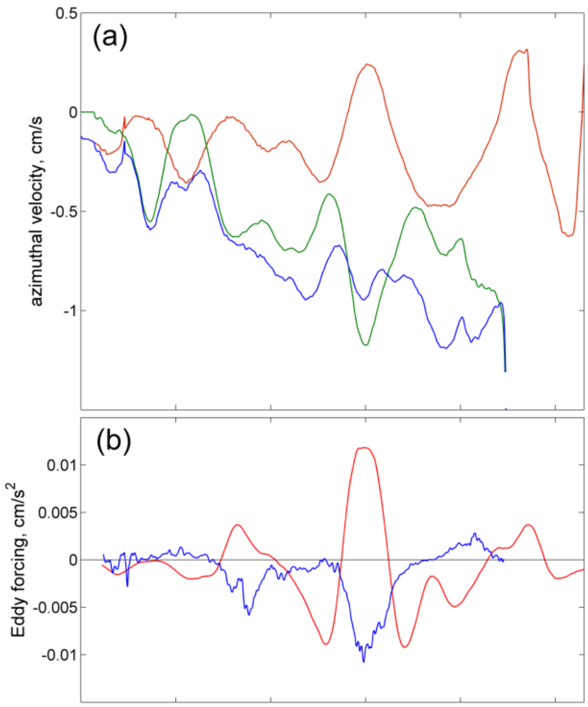

Figure 3. Profiles of the azimuthal velocity, eddy forcing and PV in the same experiment as in Figure 5: (a) radial profiles of the azimuthal barotropic/upper layer velocity $u_1 = U$ (red), azimuthal baroclinic velocity U_{bc} (green) and azimuthal lower layer velocity $u_2 = U + U_{bc}$ (blue); (b) azimuthal component of the Reynolds stress (red) and the form drag (blue) forcing in the upper layer.

Let us consider the eddy forcing components using one particular experiment with S = 45 ppt as an example. Apart from the coastal jet, at least two prominent eastward jets can be identified. Barotropic velocity profile (red in Figure 3 a) shows a strong jet at $r \approx 30$ cm as well as weaker jets in the interior and a strong coastal jet near the wall. The baroclinic velocity (green) is almost a mirror reflection of the barotropic one. The profile of the lower layer velocity (blue) which is given by the sum of the barotropic and baroclinic components indicates, however, that there are no prominent jets in the lower layer. The jets are weaker there and somewhat narrower in the meridional direction. They are imbedded in the anticyclonic mean circulation which is approximately solid-body type in the interior of the domain. Panel b in

Figure 3 shows a balance of the eddy forcing components given by the terms in the RHS of Eq. (4) in the upper layer. The Reynolds stress (red) is the main driving component; it correlates very well with the azimuthal velocity in the upper layer. The Reynolds stress is approximately balanced by the form drag. The form drag is negatively correlated with the Reynolds stress but is somewhat smaller in magnitude. The residual of the sum of these two stresses is most likely balanced by viscosity. Note that eddy forcing in the coastal jet is much weaker than that in the interior jets which indicates that their dynamics is different.

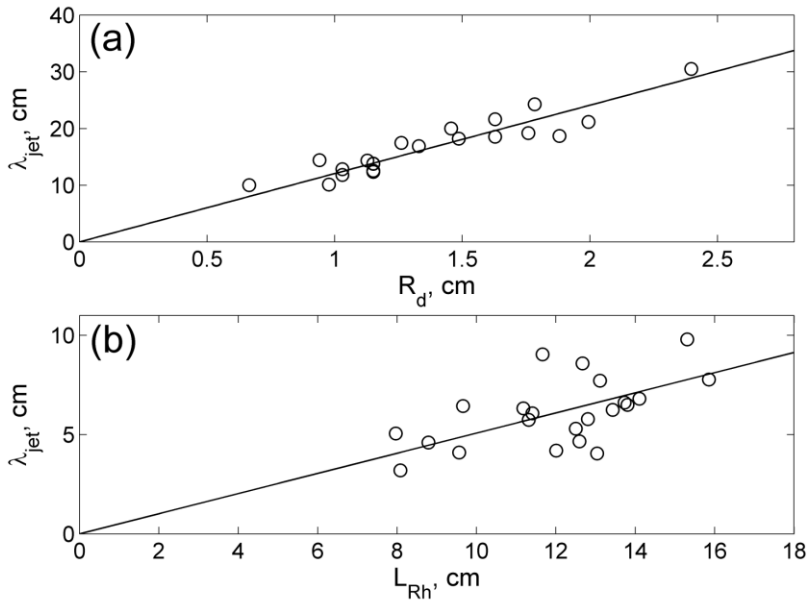

Figure 4. Characteristics of the flows measured in all experiments: (a) meridional wavelength, λ_{jet}, of zonal jets (black circles) as function of R_d; (b) λ_{jet} (black circles) as a function of the modified Rhines scale, L_{Rh}.

The meridional wavelength, λ_{jet}, of zonal jets was measured in a statistically steady regime in all experiments. The wavelength was only measured in mid-latitudes of the domain in order to exclude the coastal jet and the polar region from the measurements. Jet scaling demonstrates a linear dependence on the baroclinic radius of deformation, $\lambda_{jet} = 4.4R_d$ (Figure 4 a). Here the baroclinic radius of deformation is defined as $R_d = (g'H_0/2)^{1/2}/f_0$. Since the jets are driven by the eddy forcing which is due to baroclinic meanders, the dependence of the jet wavelength on R_d is not unexpected. However, there is another control parameter in the flow that should determine the jet scale. This parameter is due to the β-effect and is given by

$$L_{\mathrm{Rh}} = 2\pi(V_{\mathrm{rms}}/\beta)^{1/2}. \qquad (7)$$

L_{Rh} is the well-known Rhines scale and was defined as a dividing length scale between an isotropic turbulence (eddies) and linear Rossby waves (Rhines 1975). This transition scale has been viewed as an estimate of the meridional scale of the jets in different flows (e.g. Vallis and Maltrud 1993). It was also shown to apply to laboratory flows where barotropic (Afanasyev and Wells 2005, Zhang and Afanasyev 2014) or baroclinic (Read et al. 2007, Slavin and Afanasyev 2012) jets were observed. Here we test the applicability of the Rhines scale as well. Taking into account that Rhines' original theory did not include a mean flow, we use the rms radial velocity, v_{rms}, instead of the total velocity to exclude the mean zonal flow. Also, a recent study (Zhang and Afanasyev 2015) shows that a translational velocity of eddies can be used to calculate the (modified) Rhines scale; in our circumstances v_{rms} provides a suitable measure of the translational velocity of baroclinic meanders and filaments which drive the zonal jets. Figure 4 b shows that the wavelength of the jets varies linearly with L_{Rh}, $\lambda_{\mathrm{jet}} = 0.51\, L_{\mathrm{Rh}}$.

From the first glance the fact that λ_{jet} is determined equally well by two control parameters might seem controversial. Indeed, one of the parameters includes β-effect (which, of course, is necessary to create jets) and the other does not. However, this simply means that certain characteristics of the baroclinically unstable flow are affected by the β-effect. The Rhines scale includes v_{rms} which is not an external control parameter but is determined by the dynamics of the flow. Thus, one can expect the dependence of the form

$$v_{rms} \sim \beta R_d^2 . \qquad (14)$$

Our data demonstrates that there is indeed a linear dependence with a coefficient of proportionality 1.5.

4. Conclusion

In our laboratory experiments we observed the formation of zonal jets in a baroclinically unstable flow. We showed that the jets are driven by eddy forcing which is provided by baroclinic meanders and filaments on the β-plane. The meridional wavelength of the jets varies linearly with the baroclinic radius of deformation. It was also found that the jet wavelength is in good agreement with the (modified) Rhines scale. This suggested a dependence of the rms radial velocity in the equilibrated baroclinically unstable flow on the parameter βR_d.

References

Y. D. Afanasyev, P. B. Rhines, and E. G. Lindahl, "Velocity and potential vorticity fields measured by altimetric imaging velocimetry in the rotating fluid," Exp. Fluids. **47**, 913 (2009).

Y. D. Afanasyev, and J. Wells, "Quasi-two-dimensional turbulence on the polar beta-plane: laboratory experiments," Geoph. Astroph. Fluid Dyn. **99**, 1 (2005).

Y. Zhang and Y. D. Afanasyev, "Beta-plane turbulence: experiments with altimetry." Phys. Fluids **26**, 026602 (2014).

Y. Zhang and Y. D. Afanasyev, "Rossby wave radiation by an eddy on a beta-plane: Experiments with laboratory altimetry," submitted to Phys. Fluids (2015).

N. A. Maximenko, B. Bang, and H. Sasaki, "Observational evidence of alternating zonal jets in the world ocean," Geoph. Res. Lett. **32**, L12607 (2005).

P. L. Read, Y. H. Yamazaki, S. R. Lewis, P. D. Williams, R. Wordsworth, K. Miki-Yamazaki, J. Sommeria, H. Didelle, and A. M. Fincham, "Dynamics of Convectively Driven Banded Jets in the Laboratory," J. Atmos. Sci. **64(11)**, 4031 (2007).

P. B. Rhines, "Waves and turbulence on a beta-plane," J. Fluid Mech. **69(3)**, 417 (1975).

A. G. Slavin, Y.D. Afanasyev, "Multiple zonal jets on the polar beta plane," Phys Fluids, 24, 016603 (2012)

A. F. Thompson, "The atmospheric ocean: eddies and jets in the Antarctic Circumpolar Current," Phil. Trans. R. Soc. A 366, 4529–4541 (2008).

G. K. Vallis, and M. E. Maltrud, "Generation of mean flows and jets on a beta-plane and over topography," J. Phys. Oceanog. **23**, 1346 (1993).